Catalytic Cycles for the Reduction of $[UO_2]^{2+}$ by Cytochrome c_7 Proteins Proposed from DFT Calculations

Mahesh Sundararajan, Andrew J. Campbell, and Ian H Hillier*

School of Chemistry, University of Manchester, Manchester M13 9PL, U.K.

Received: January 9, 2008; Revised Manuscript Received: February 15, 2008

The mechanism of the reduction of the hydrated uranyl cation, $[UO_2]^{2+}$, by the cytochromes *G. sulfurreducens* and *D. acetoxidans* has been studied using density functional theory calculations. We propose that the initial electron transfer step from the heme is to a cation−cation complex in the case of *D. acetoxidans*, but for *G. sulfurreducens*, it is to a single uranyl cation, which then forms a U(V)−U(VI) complex with a second uranyl cation. For both enzymes, the subsequent catalytic pathways are very similar. A U(V)−U(V) complex is formed, which then undergoes disproportionation via two successive protonation steps of one uranyl group, to give a U(VI)−U(IV) complex which dissociates to individual U(VI) and U(IV) species, the former being bound at the enzyme active site. Intermediate structures along the catalytic pathway are consistent with EXAFS data.

1. Introduction

The chemistry of uranium and other transuranics, and of their complexes, is receiving increased attention at the present time due to the environmental danger posed by such species.[1–4] One possible way to control their release into groundwater is to take advantage of the differing solubility of the different oxidation state. Strategies for reducing the mobility of these species usually center on their reduction to less soluble, lower oxidation state species, in the case of uranium reducing soluble U(VI) to insoluble U(IV).[2,3] This process is facilitated by iron containing mineral surfaces and by multi-heme cytochromes.[4–6] These cytochromes which occur in the periplasm of Fe(III) reducing bacteria and in sulfur and sulfate reducing bacteria can play critical roles in the environmental processing of many metals, including radionuclides.[6] One such cytochrome, a c_7 from *Geobacter sulfurreducens* (*G. sulfurreducens*), often known as PpcA, is a protein with 71 amino acid residues that contains three covalently bound hemes.[7] The purified protein can reduce U(VI), Cr(VI), and other metal ions.[5] It is one of the smallest *c*-type cytochromes with the highest ratio of hemes to amino acid residues. The chromate binding site was identified by NMR methods for the homologous cytochrome c_7 from *Desulfuromonas acetoxidans* (*D. acetoxidans*),[6] the structure of which was determined by X-ray diffraction. Both *G. sulfurreducens* and *D. acetoxidans* are effective in reducing metal ions, but the mechanism of this process is far from clear.[7] In general terms, the multiple heme centers of c_7 cytochromes can provide pathways for successive electron transfers to surface bound metal species.[8] The design of potentially useful enzyme mimics would be helped if the structurally important features of the reduction mechanism were known.

In recent years, there has been a large increase in the computational study of actinide complexes, particularly those of uranium,[9–18] but there is less work on those of neptunium[14,17,19,20] and plutonium.[12,14,17] The electronic structure and molecular geometry of the di-oxo cation of these three elements have been studied at the Hartree Fock (HF),[12] density functional theory (DFT),[13–17] and correlated *ab initio* levels.[14,19] Theoretical studies have also modeled complexes of these cations, especially uranyl, using various methods for the inclusion of aqueous solvation effects including both variants of continuum models and by explicitly including the solvent molecules.[13,14,17,18] The changes in the geometric and electronic structures of these complexes upon reduction (M(VI) to M(V)) have also been studied due to their relevance to the reduction process. It is well known that following the reduction of U(VI) to U(V), the U(V) species then undergoes a disproportionation reaction under acidic conditions, which has recently been studied using DFT calculations by Steele and Taylor.[21] We compare our mechanism with these calculations later in this paper.

There are also an increasing number of studies related to the redox chemistry of actinyl complexes, aimed at predicting the redox potentials, and more recently the kinetics of the electron transfer process accompanying reduction. The importance of spin-orbit effects and solvation on the calculation of the rate of electron transfer of uranium (VI/V)[9] and neptunium (VI/V)[11] has been discussed. Similarly, Wander et al. have studied the kinetics of electron transfer between aqueous ferrous iron and a triscarbonato uranyl species.[22]

In this paper, we here describe the first computational study to predict a catalytic cycle for the enzymatic reduction of the uranyl cation, $[UO_2]^{2+}$ (U(VI) to (U(IV)), by both *G. sulfurreducens* and *D. acetoxidans*.

2. Computational Strategy

Our computational strategy is to identify the binding site of the enzyme for the uranyl cation, and to use these structures as starting points to generate realistic models for DFT calculations of the structures and energetics of species which we predict to occur along possible pathways for reduction. We here focus on the electron transfer from the iron center and the subsequent reduction of the bound uranyl cation. We do not discuss how the oxidized heme is subsequently reduced by the electron sink, which is part of the complete catalytic cycle.

(a) Uranyl Binding Site. The binding site of $[UO_2]^{2+}$ in the c_7 cytochrome of *D. acetoxidans* was identified using the

* Corresponding author. Phone: (+44) 161 275 4686. Fax: (+44) 161 275 4734.

10.1021/jp800209p CCC: $40.75
Published on Web 04/03/2008

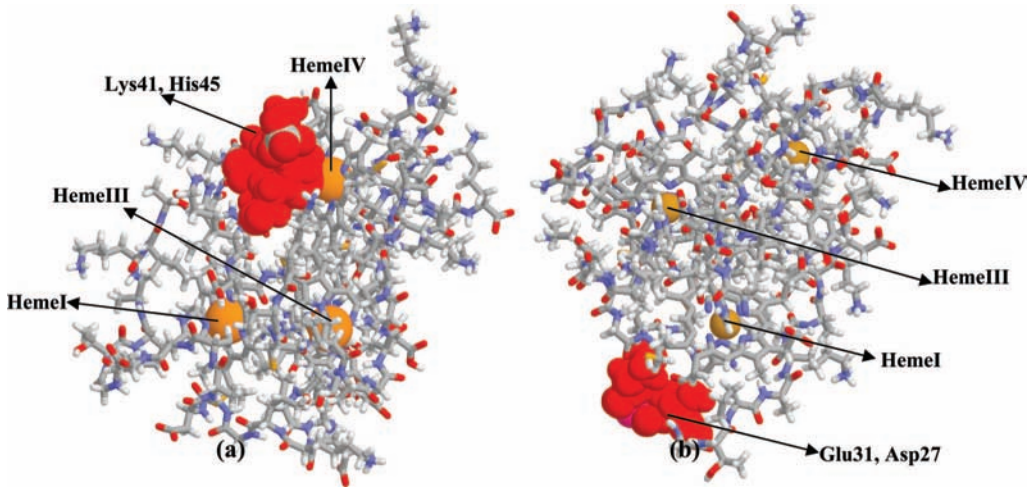

Figure 1. Binding sites of (a) CrO_4^{2-} and (b) UO_2^{2+} for *D. acetoxidans* c_7 cytochrome.

TABLE 1: Structures (Å) and Spin State Energies (kcal mol^{-1}) of bis-Imidazole Iron (II) Porphyrin [Fe−P−(Im$_2$)]^0

	B3LYP			BP86		
	Fe−N$_{por}$	Fe−N$_{Im}$	relative energy in H_2O ($CHCl_3$)	Fe−N$_{por}$	Fe−N$_{Im}$	relative energy in H_2O ($CHCl_3$)
$S = 0$	2.01–2.02	2.01	0.0 (0.0)	2.00	1.97	0.0 (0.0)
$S = 1$	2.01–2.02	2.00	+21.1 (+21.9)	2.01–2.02	1.97	+18.6 (20.7)
$S = 2$	2.07–2.08	2.31	+7.6 (+7.7)	2.07–2.08	2.25	+32.0 (32.0)

Autodock program,[23] which is based on a molecular mechanical force field to model the substrate−protein interactions using a genetic algorithm for global searching. The reliability of this docking program is well documented in the literature, and it is one of the most popular and frequently used docking software.[24] We have taken the NMR structure of *D. acetoxidans* (PDB code 1EHJ)[6] for which the protonation states of amino acid residues are known and searched for the optimal binding site for $[UO_2]^{2+}$. The search covered the entire enzyme with a population of 750 and with the crossover rate, mutation rate, and elitism set at default values of 0.8, 0.2, and 1, respectively.

In the resulting docked structure, we find that $[UO_2]^{2+}$ is bound to the only two negatively charged residues in close proximity to each other, Asp27 and Glu31, ~11 Å away from heme I. Glu31 is directly attached to His30 which in turn is coordinated to heme I (Figure 1b). This finding is in line with an assessment of crystallographic data from the Protein Data Bank, for the biocoordination of the uranyl cation. This shows that carboxylate donors from aspartate, glutamate, or the carboxyl terminus in proteins make up the majority of inner-sphere interactions with this cation.[25] In the case of *G. sulfurreducens* (PDB code 1OS6),[7] there are not two carboxylate groups in close proximity, and hence, we chose Glu31 (in 1OS6, it is Glu32) as the sole binding site, which is in close proximity to heme I.

To verify this strategy, we have docked the chromate di-anion (CrO_4^{2-}) to *D. acetoxidans*, the experimental binding site being known for the sulfate di-anion.[7] In agreement with this result, we find chromate to be bound near heme IV, the di-anion being anchored by His45 and Lys41 (Figure 1a), which gives us confidence in our docking strategy.

We now use the uranyl docked structure as the starting point to generate initial structures to explore the following aspects of the reduction mechanism.

(i) How facile is the initial electron transfer from the heme center to the docked uranyl?

(ii) How does the subsequent disproportionation of U(V) take place; in particular, what is the role of the enzyme residues in this process?

(iii) Is there any difference in the reduction mechanism for the two cytochromes, *D. acetoxidans and G. sulfurreducens*?

(b) Quantum Mechanical Cluster Calculations. It is traditional to use DFT methods to describe large metal complexes, but there is the ever-present problem of choosing the most appropriate functional, with both B3LYP and BP86 having been used by other workers.[13,17,21] These and other functionals have generally been considered adequate when judged against experimental structures and high level *ab initio* calculations. We here use mainly the BP86 functional[26] but also see if the use of the B3LYP functional affects our conclusions. Structures were optimized using an SDD small core relativistic pseudopotential[27] with a segmented contracted Gaussian basis [10s, 9p, 5d, 4f] for U, and a 6–31G* basis for the remaining atoms, which we denote basis B1. The small core SDD basis has been found to successfully predict structures and vibrational frequencies for a number of uranium complexes.[17,28] The energies of these structures are also evaluated using a larger basis (B2) which is expanded to 6–311+G** on all ligand atoms. The effect of the condensed phase environment was modeled using the polarizable continuum model (C-PCM),[29] using a dielectric of 4.9 to simulate the protein environment or 78.39 to simulate bulk water. Calculations were carried out using Gaussian 03[30] and the structures characterized as minima by calculation of harmonic frequencies. All open shell calculations were for the high spin state.

3. Computational Results

(i) Electron Transfer from Heme. We first investigate the use of basis B1 to determine the structure and spin state of the heme center using the isolated bis-imidazole iron(II) porphyrin model [Fe−P(Im)$_2$]^0. The structures were evaluated using both BP86 and B3LYP functionals, and the energies were subse-

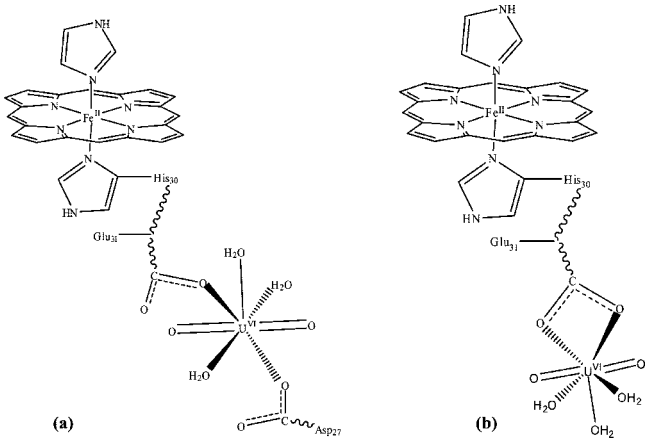

Figure 2. $[UO_2]^{2+}$ bound to heme I in (a) *D. acetoxidans* and (b) *G. sulfurreducens*.

quently determined including bulk effects using the C-PCM model (Table 1). We find that both functionals favor the singlet state compared to the triplet or quintet state which is consistent with experimental data for *D. acetoxidans*.[6] Since the bound $[UO_2]^{2+}$ ion is ~11 Å away from the heme I, it is expected to have little effect on the relative energies of the spin states of the heme.

(ii) Reduction of Bound Uranyl. We now turn to the structure and redox properties of the $[UO_2]^{2+}$ complex bound near heme I for both *D. acetoxidans* and *G. sulfurreducens*. Complexes of $[UO_2]^{2+}$ are usually found with five equatorial ligands, some of which are often water molecules. For example, uranyl mono-carboxylate complexes $\{[UO_2(OOCR)(H_2O)_n]^+$, $n = 3$ or $4\}$ have recently been studied by Schlosser et al.,[31] who found both mono- and bi-dentate structures to be possible and are very close in energy. In *G. sulfurreducens*, we have taken the bi-dentate structure, but for *D. acetoxidans*, we have investigated both mono- and bi-dentate motifs, the results which we now first describe being for the mono-dentate structure. In the models of bound $[UO_2]^{2+}$ for the two different enzymes, we have included three additional water molecules, in addition to the carboxylate ligand(s), to give a seven-coordinate species, as shown in Figure 2. We have optimized these models of the U(VI) complex bound to the heme (Figure 2) to first see whether the details of the structures of the bound uranyl complexes for the two enzymes differ from those of the corresponding isolated complexes $[UO_2(CH_3COO)_n(H_2O)_3]$, $n = 1, 2\ ]^{2-n}$ which we have also determined. We note that this complex is neutral when $n = 2$, corresponding to *D. acetoxidans* but has a single positive charge when $n = 1$ (*G. sulfurreducens*). The structures are compared in Table 2, where we see that the presence of heme I has very little effect on the geometry of the bound uranyl complex. We also see that the U−O (axial) lengths are similar (1.80 Å) for both *D. acetoxidans* and *G. sulfurreducens*. Our optimized axial and equatorial uranyl lengths are in good ageement with the X-ray data reviewed by Horn and Huang.[25a]

We have taken our optimized *D. acetoxidans* and *G. sulfurreducens* models (Figure 2) involving both the heme and the uranyl complex and estimated the electron transfer energy (Fe(II)−U(VI) → Fe(III)−U(V)). Due to difficulties in optimizing the structure of the open shell singlet state [Fe(III)−U(V)], we have taken the closed shell singlet structure [Fe(II)−U(VI)] to evaluate the energy of the [Fe(III)−U(V)] state, thus corresponding to a vertical electron transfer process. We find that for the neutral uranyl complex (*D. acetoxidans*) electron transfer is unfavorable by 47 kcal mol^{-1} and is now slightly favorable, by 3 kcal mol^{-1}, for the singly charged complex (*G. sulfurreducens*), both with a bulk dielectric of 78.39. To estimate the effect of not allowing either the electron donor (heme) or acceptor to relax upon electron transfer, we have evaluated the relaxation energies of the two component systems individually. We find that the value for the heme is 1 kcal mol^{-1} and for the uranyl complexes is 5 or 4 kcal mol^{-1} for the complex with two and one acetate ligands, respectively. The inclusion of the effects of spin-orbit coupling in the U(V) species (~7 kcal mol^{-1})[16] and of structural relaxation of the electron donor and acceptor groups thus do not change the conclusion that electron transfer to the U(VI) species is unfavorable for *D. acetoxidans*, but it is now more favorable for *G. sulfurreducens*.

These calculations suggest that the role of the carboxylate amino acid residues is central in modulating the electron transfer to the uranyl center. In our models, for *D. acetoxidans* cytochromes, uranyl is coordinated to both Asp27 and Glu31 residues, whereas, in *G. sulfurreducens*, only a single Glu residue coordinates to the UO_2 moiety, the remaining sites being filled by three water molecules. Thus, the stabilization of the U(VI) species by the carboxylate ligands is greater for *D. acetoxidans* than for *G. sulfurreducens*. Our calculations suggest that it is not favorable to form an initial U(V) species in the case of *D. acetoxidans*, so that a mechanism involving the disproportionation of two individually formed U(V) species is unlikely, and this has led us to explore an alternative reduction mechanism which involves a second $[UO_2]^{2+}$ species approaching the first surface bound uranyl cation of Figure 1b, and which can lead to a final U(VI)−U(IV) structure. However, since in the case of *G. sulfurreducens* an initial U(V) species is formed, a different reduction mechanism is suggested for the two closely related enzymes. We now discuss calculations to explore possible enzymatic reduction mechanisms.

To focus on the uranyl center, we employ a model in which $[UO_2]^{2+}$ is coordinated to two acetate groups to mimic Asp27 and Glu31 for *D. acetoxidans* and one acetate group to mimic Glu32 for *G. sulfurreducens*, as well as to a number of water molecules (Figures 3 and 4). We find that, for the *D. acetoxidans* model, a

TABLE 2: Structures (Å) of Isolated and Enzyme Bound Models of *D. acetoxidans* and *G. sulfurreducens*

	D. acetoxidans			*G. sulfurreducens*		
	isolated model		enzyme bound model	isolated model		enzyme bound model
	$[Fe-P(Im)_2]^0$	$[UO_2(CH_3COO)_2\text{-}(H_2O)_3]^0$	$[Fe-P(Im)_2-[UO_2(Glu, Asp)(H_2O)_3]^0$	$[Fe-P(Im)_2]^0$	$[UO_2(CH_3COO)\text{-}(H_2O)_3]^{1+}$	$[Fe-P(Im)_2-[UO_2(Glu)(H_2O)_3]^{1+}$
$Fe-N_{por}$	2.00		1.99–2.00	2.00		2.00
$Fe-N_{Im}$	1.97		1.95–1.99	1.97		1.96
U−O		1.80–1.81	1.80		1.79	1.79
$U-O_{CH_3COO}$		2.29–2.40	2.34–2.35		2.35–2.36	2.36–2.37
$U-O_{H_2O}$		2.45–2.59	2.44–2.47		2.49–2.51	2.48–2.51

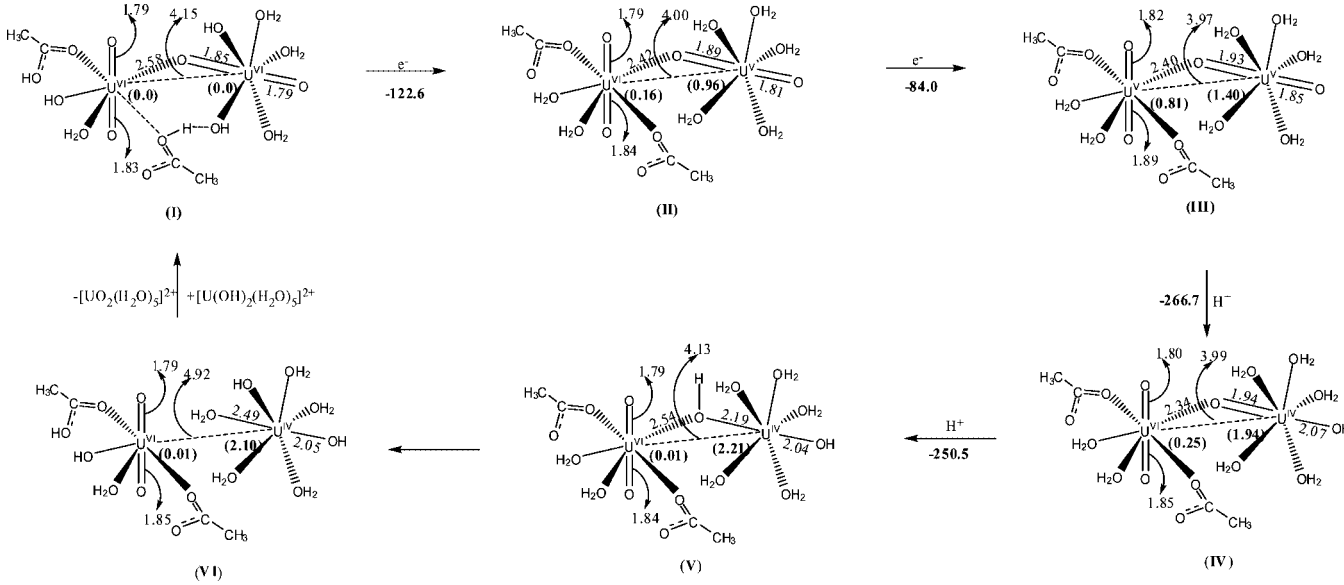

Figure 3. Reaction pathway for the bioreduction of $[UO_2]^{2+}$ in *D. acetoxidans*. Bond lengths (Å), relative energies (kcal mol^{-1}), and Mulliken spin densities (in parentheses) are shown.

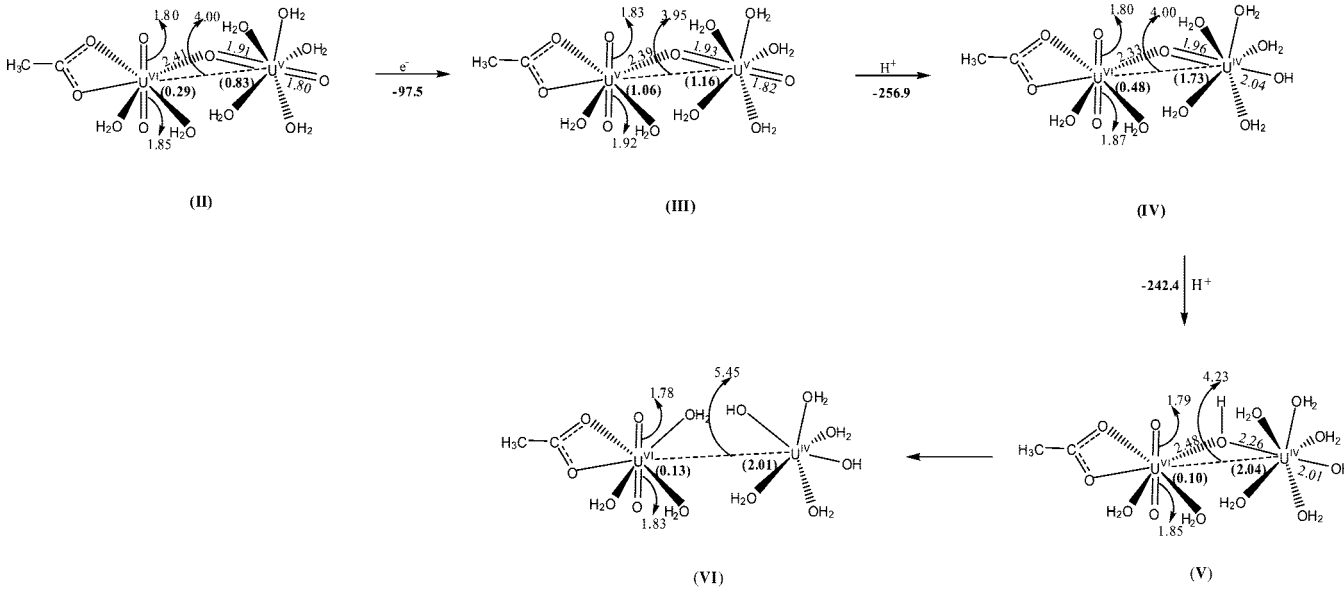

Figure 4. Reaction pathway for the bioreduction of $[UO_2]^{2+}$ in *G. sulfurreducens*. Bond lengths (Å), relative energies (kcal mol^{-1}), and Mulliken spin densities (in parentheses) are shown.

second hydrated $[UO_2]^{2+}$ species can displace one of the water molecules from the first bound $[UO_2]^{2+}$ entity, to form a T-shaped cation−cation complex (Figure 3, **I**), in which proton transfer has occurred to both acid groups, one such proton being from the second $[UO_2]^{2+}$ complex. This structure has been identified as a minimum, and its binding energy is calculated as the difference in the zero-point corrected energies for the following reaction: $[UO_2(CH_3COO)_2(H_2O)_3]^0 + [UO_2(H_2O)_5]^{2+} \rightarrow [U_2O_4(CH_3COO)_2(H_2O)_7]^{2+} + H_2O$.

With the inclusion of bulk solvation, the binding energy was found to be slightly unfavorable (by 1.5 kcal mol^{-1}), but we find that such a di-nuclear species does support an additional electron, the electron affinity of (**I**) being 122.6 kcal mol^{-1}, which is significantly greater than the value for $[UO_2(COOCH_3)_2(H_2O)_3]$ (by 46 kcal mol^{-1}) and is also greater (by 32 kcal mol^{-1}) than our estimate of the ionization energy of the heme (90 kcal mol^{-1}). We find that, in the U(VI)−U(V) species ((**II**), Figure 3), the added electron resides on the second hydrated $[UO_2]^{2+}$ group which we now designate electron acceptor, rather than the initial $[UO_2]^{2+}$ coordinated to the two acid groups, which we label electron donor.

Attempts were made to form a similar U(VI)−U(VI) species for the *G. sulfurreducens* model but without success. In this case, upon geometry optimization, the structure dissociated into two individual U(VI) species, again suggesting a different mechanism for *G. sulfurreducens*.

We now follow further reduction of the U(VI)−U(V) species (**II**) formed by electron transfer to the transient U(VI)−U(VI) species that we have identified for *D. acetoxidans*, and disproportionation of the resulting U(V)−U(V) species. In (**II**) (Figure 3), each acetate group has lost a proton to regenerate the original water molecules. Further reduction of (**II**), by addition of a second electron, is favored by 84.0 kcal mol^{-1} and results in the U(V)−U(V) structure (**III**), which then undergoes disproportionation.

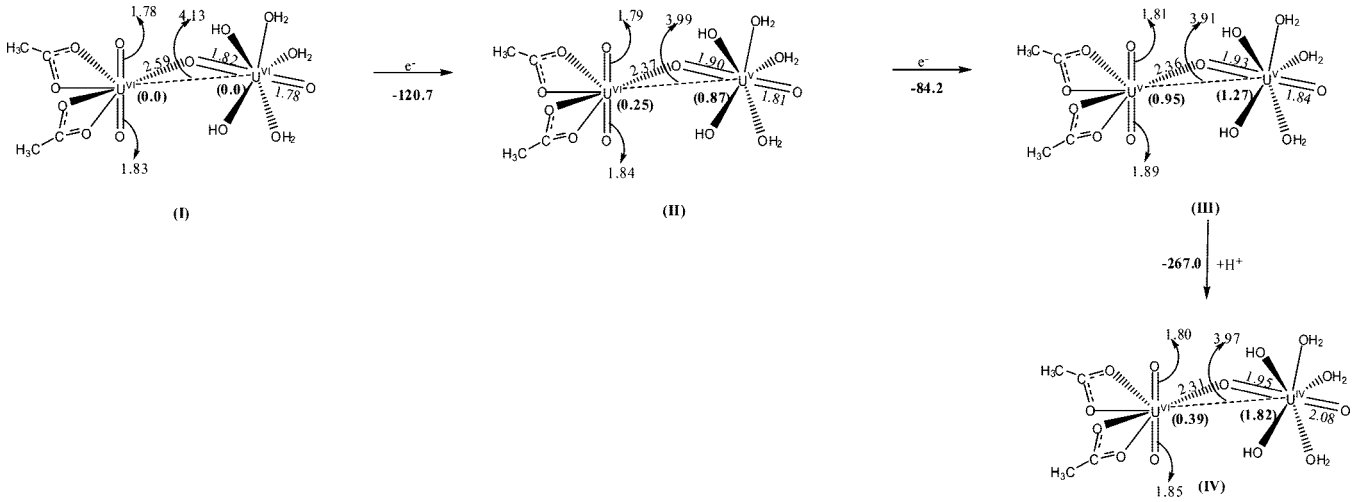

Figure 5. Reaction pathway for the bioreduction of $[UO_2]^{2+}$ in the bi-dentate mode of *D. acetoxidans*. Bond lengths (Å), relative energies (kcal mol^{-1}), and Mulliken spin densities (in parentheses) are shown.

TABLE 3: Energies (kcal mol^{-1}) of the Steps[a] Involved in the Disproportionation Mechanism of *D. acetoxidans*

species	BP86/B1 ($\varepsilon = 1$)	BP86/B1 ($\varepsilon = 4.9$)	BP86/B1 ($\varepsilon = 78.39$)	B3LYP/B1 ($\varepsilon = 78.39$)	BP86/B2 ($\varepsilon = 78.39$)
(**I**)−(**II**)	−214.2	−140.5	−122.6	−129.0	−128.5
(**II**)−(**III**)	−116.1	−90.8	−84.0	−95.1	−91.2
(**III**)−(**IV**)	−234.3	−259.7	−266.7	−260.1	−267.8
(**IV**)−(**V**)	−153.9	−231.2	−250.5	−262.0	−251.4

[a] See Figure 3.

In the case of the *G. sulfurreducens* complex, the mono-acetate model (Figure 4), a similar structure (**II**) is formed by addition of a second U(VI) species to the initially formed U(V) species. We find that the formation of such a complex is favorable (by 5.8 kcal mol^{-1}) and that the structure, particularly the U−U distance, as well as the spin densities (asymmetric) are very similar for this structure (**II**) for both enzyme models.

(iii) Disproportionation Mechanism. Before discussing the actual disproportionation mechanism for the two enzyme models, we note that there are differences in the electronic structure of the two models of the U(V)−U(V) species. The spin densities on the two uranium atoms are more asymmetric in the di-acetate than in the mono-acetate model which suggests that the former model is more ready to disproportionate. It is well known that the disproportionation process occurs at low pH (<7),[5] and we do find that protonation of (**III**) is necessary for this to occur. We find that such protonation occurs preferentially at the terminal oxygen of (**III**) and completes the electron transfer to give the species (**IV**) for both models, in which the spin density is strongly localized on one uranium (U(IV)) atom. The cleavage of the bridging U(VI)−O bond in (**IV**) to finally release the hydrated U(IV) species requires protonation of the bridging oxygen atom of (**IV**), to give initially (**V**) in which essentially all the spin density now resides on the hydrated acceptor group (Figures 3 and 4). The energies associated with the protonation of (**III**) and (**IV**) are close to the solvation free energy of the proton (264 kcal mol^{-1})[32] for the *D. acetoxidans* model and slightly unfavorable (257 kcal mol^{-1}) for the *G. sulfurreducens* model. The somewhat smaller value for the protonation energy of (**IV**) to form (**V**) compared to the corresponding value for the protonation step (**III**) to form (**IV**) may indicate that the former is the rate determining step in the reduction.

The final step needed to cleave the U(IV)−U(VI) bond and thus to regenerate the bound U(VI) species is an internal proton transfer from a coordinated water molecule of the acceptor of (**V**) to the bridging −OH group. This step completes the catalytic cycle, and the bound U(VI) species can now continue the reduction process via the formation of (**I**) in *D. acetoxidans* and via (**II**) in *G. sulfurreducens*.

We have investigated whether a number of aspects of our calculations affect our proposed mechanisms. Firstly, we have performed calculations with the *D. acetoxidans* model having bi-dentate rather than mono-dentate carboxylate ligands. In Figure 5, we report the corresponding structures and relative energies of the species from (**I**) to (**IV**). In both coordination modes, the geometric features and the associated energetics are very similar (Figures 3 and 5) which indicates both mono-dentate and bi-dentate motifs are equally possible, as also suggested by Schlosser et al.[31] for the mono-carboxylate complex of $[UO_2]^{2+}$. To investigate the possible importance of a larger basis set, we have computed the energetics using BP86/B1 structures (Table 3) in conjunction with the larger basis, B2, and find that our conclusions are unchanged. Furthermore, the use of the B3LYP functional, rather than BP86, with the BP86/B1 structures and thermodynamic corrections, has only a marginal effect on the relative energies (Table 3). We find that the formation of (**II**) and (**III**) is more favorable compared to BP86/B1, but the actual disproportionation product (**IV**) is somewhat less favorable (Table 3). Finally, we have investigated the use of the protein dielectric ($\varepsilon = 4.90$), rather than the value for bulk water ($\varepsilon = 78.39$). Use of the protein dielectric indicates that the formation of (**II**) and (**III**) is more favorable than in bulk water and that the actual disproportionation product (**IV**) is somewhat less favorable (Table 3). As the binding site is surface exposed, we might expect the dielectric constant near the enzyme surface (water dielectric) to be somewhat higher than the value inside the protein (chloroform dielectric).

A U(V) disproportionation mechanism of uranyl aqua complexes has been proposed by Steele and Taylor[21] based upon calculated structures along the reaction pathway. This mechanism proceeds via the formation of a cation−cation complex,

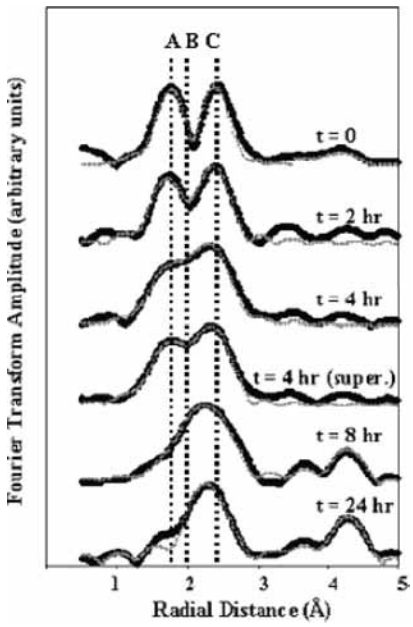

Figure 6. EXAFS spectrum. Reprinted from ref 5 with permission. Copyright 2005 American Chemical Society.

followed by two successive protonations of the axial oxygens of one uranyl center. They find that electron transfer is complete after the first protonation, which involves the bridging oxygen atom, and that the resulting U(VI)−U(IV) complex is dissociated by the addition of a further water molecule. Although there are similarities with the latter stages of our proposed mechanisms (Figures 4−6), the presence of the carboxylate groups is responsible for a number of differences. Thus, initial protonation which is accompanied by electron transfer occurs at the terminal oxygen of structure (**III**), and the final dissociation of the complex occurs via an internal proton transfer.

We can make contact with experiment via an EXAFS study[5] of the reduction of $[UO_2]^{2+}$ by *G. sulfurreducens* which has revealed progressive changes in the spectrum over a 24 h period (Figure 6) which are consistent with the changes in the U═O axial and U−U distances along our predicted reaction pathway for both enzyme models studied here. The major changes are the gradual growth of a peak at ∼2.1 Å and the loss of one at ∼1.8 Å, corresponding to the elongation of the U═O axial bond upon reduction (Figures 3 and 4), and the appearance of a peak at ∼3.8 Å followed by one at ∼4.2 Å. These changes are in line with our predicted mechanism. Thus, initially, no U−U peak is observed, since (**I**) is only a transient complex in *D. acetoxidans* and it does not form in *G. sulfurreducens*. We propose that the U(V)−U(V) species (**III**), with a predicted U−U separation of 4.00 Å (3.95 Å) corresponds to the structure which appears after ∼2 h, while the final structure at 24 h is dominated by the U(VI)−U(IV) species (**V**) having a U−U distance of 4.13 Å (4.23 Å) for *D. acetoxidans* (*G. sulfurreducens*) enzyme models.

4. Conclusions

In this paper, we have addressed various issues concerning the enzymatic reduction mechanism of $[UO_2]^{2+}$ by both *D. acetoxidans* and *G. sulfurreducens* cytochrome c_7 proteins. We propose that both enzymes can catalyze the reduction of uranyl (U(VI)) but by slightly different mechanisms, which is due to the number of carboxylate amino acid residues bound to the UO_2^{2+} species. Thus, for *D. acetoxidans*, both carboxylate residues, Asp27 and Glu31, are bound to the substrate cation which results in electron transfer from the heme being energetically unfavorable, and requires the binding of a second substrate molecule to form a weak cation−cation complex which can accept an electron from the heme. However, in the case in *G. sulfurreducens*, the $[UO_2]^{2+}$ substrate is bound to a single carboxylate group, and can support an electron from the heme before interaction with a second hydrated substrate molecule occurs. For both enzymes, a U(V)−U(V) complex is subsequently formed which undergoes disproportionation via two protonation steps involving the axial oxygens of one U(V) center. We find that structures along our proposed pathway are consistent with EXAFS data.[5] Thus, these calculations provide new structural and mechanistic insight into the way in which cytochrome bioreduction of $[UO_2]^{2+}$ could take place via a disproportionation pathway in both *D. acetoxidans* and *G. sulfurreducens* cytochrome c_7 proteins.

Acknowledgment. We thank the Leverhulme Trust for financial support and the North West Development Agency (NWDA) for the provision of the NW Grid computing facility. We also thank Professors F. R. Livens and J. R. Lloyd for helpful discussions.

Supporting Information Available: Coordinates of optimized structures, C-PCM energies corrected for zero-point energies, and $\langle S^2 \rangle$ value of wavefunction, for species II−VI (Figure 3). This material is available free of charge via the Internet at http://pubs.acs.org.

References and Notes

(1) Katz, J. J.; Morss, L. R.; Seaborg, G. T. *The Chemistry of the Actinide Elements*, 2nd ed.; Chapman and Hall: London, 1986.
(2) Anderson, R. T.; Vrionis, H. A.; Ortiz-Bernad, I.; Resch, C. T.; Long, P. E.; Dayvault, R.; Karp, K.; Marutzky, S.; Metzler, D. R.; Peacock, A.; White, D. C.; Lowe, M.; Lovley, D. R. *Appl. Environ. Microbiol.* **2003**, *69*, 5884.
(3) Lovley, D. R.; Phillips, E. J. P.; Gorby, Y. A.; Landa, E. *Nature* **1991**, *350*, 413.
(4) Lovley, D. R.; Roden, E. E.; Phillips, E. J. P.; Woodward, J. C. *Marine Geol.* **1993**, *113*, 41.
(5) Renshaw, J. C.; Butchins, L. J. C.; Livens, F. R.; May, I.; Charnock, J. M.; Lloyd, J. R. *Environ. Sci. Technol.* **2005**, *39*, 5657.
(6) Assfalg, M.; Bertini, I.; Bruschi, M.; Michel, C.; Turano, P. *Proc. Natl. Acad. Sci. U.S.A.* **2002**, *99*, 9750.
(7) Pokkuluri, P. R.; Londer, Y. Y.; Duke, N. E. C.; Long, W. C.; Schiffer, M. *Biochemistry* **2004**, *43*, 849.
(8) Mowat, C. G.; Chapman, S. K. *Dalton Trans.* **2005**, 3381.
(9) Vallet, V.; Macak, P.; Walgren, U.; Grenthe, I. *Theor. Chem. Acc.* **2006**, *115*, 146.
(10) Sarrio, C. C.; Vallet, V.; Maynau, D.; Marsden, C. Y. *J. Chem. Phys.* **2004**, *121*, 5312.
(11) Privalov, T.; Macak, P.; Schimmelpfennig, B.; Fromager, E.; Grenthe, I.; Wahlgren, U. *J. Am. Chem. Soc.* **2004**, *126*, 9801.
(12) Craw, J. S.; Vincent, M. A.; Hillier, I. H.; Wallwork, A. L. *J. Phys. Chem. A* **1995**, *99*, 10181.
(13) Kaltsoyannis, N. *Coord. Soc. Rev.* **2003**, *32*, 9.
(14) Cao, Z.; Balasubramanian, K. *J. Chem. Phys.* **2005**, *123*, 114309.
(15) de Jong, W. A.; Apra, E.; Windus, T. L.; Nichols, J. A.; Harrison, R. L.; Gutowski, K. E.; Dixon, D. A. *J. Phys. Chem. A* **2005**, *109*, 11568.
(16) Hay, P. J.; Martin, R. L.; Schreckenbach, G. *J. Phys. Chem. A* **2000**, *104*, 6259.
(17) Shamov, G. A.; Schreckenbach, G. *J. Phys. Chem. A* **2005**, *109*, 10961.
(18) Buhl, M.; Diss, R.; Wipff, G. *J. Am. Chem. Soc.* **2005**, *127*, 13506.
(19) Gagliardi, L.; Roos, B. O. *Inorg. Chem.* **2002**, *41*, 1315.
(20) Macak, P.; Fromager, E.; Privalov, T.; Schimmelpfennig, B.; Grenthe, I.; Wahlgren, U. *J. Phys. Chem. A* **2005**, *109*, 4950.
(21) Steele, H.; Taylor, R. J. *Inorg. Chem.* **2007**, *46*, 6311.
(22) Wander, M. C. F.; Kerisit, S.; Rosso, K. M.; Schoonen, M. A. A. *J. Phys. Chem. A* **2006**, *110*, 9691.
(23) Morris, G. M.; Goodsell, D. S.; Halliday, R. S.; Huey, R.; Hart, W. E.; Belew, R. K.; Olson, A. J. *J. Comput. Chem.* **1998**, *19*, 1639.

(24) Goodsell, D. S.; Morris, G. M.; Olson, A. J. *J. Mol. Recognit.* **1996**, *9*, 1.

(25) (a) van Horn, J. D.; Huang, H. *Coord. Chem. Rev.* **2006**, *250*, 765. (b) Golovin, A.; Dimitropoulos, D.; Oldfield, T.; Rachedi, A.; Henrick, K. *Proteins* **2005**, *58*, 190.

(26) Perdew, J. P. *Phys. Rev. B* **1986**, *33*, 8822.

(27) Cao, X.; Dolg, M. *THEOCHEM* **2004**, *673*, 203.

(28) Schreckenbach, G.; Hay, P. J.; Martin, R. L. *J. Comput. Chem.* **1999**, *20*, 70.

(29) Barone, V.; Cossi, M. *J. Phys. Chem. A* **1998**, *102*, 1995.

(30) Frisch, M. J.; Trucks, G. W.; Schlegel, H. B.; Scuseria, G. E.; Robb, M. A.; Cheeseman, J. R.; Montgomery, J. A., Jr.; Vreven, T.; Kudin, K. N.; Burant, J. C.; Millam, J. M.; Iyengar, S. S.; Tomasi, J.; Barone, V.; Mennucci, B.; Cossi, M.; Scalmani, G.; Rega, N.; Petersson, G. A.; Nakatsuji, H.; Hada, M.; Ehara, M.; Toyota, K.; Fukuda, R.; Hasegawa, J.; Ishida, M.; Nakajima, T.; Honda, Y.; Kitao, O.; Nakai, H.; Klene, M.; Li, X.; Knox, J. E.; Hratchian, H. P.; Cross, J. B.; Bakken, V.; Adamo, C.; Jaramillo, J.; Gomperts, R.; Stratmann, R. E.; Yazyev, O.; Austin, A. J.; Cammi, R.; Pomelli, C.; Ochterski, J. W.; Ayala, P. Y.; Morokuma, K.; Voth, G. A.; Salvador, P.; Dannenberg, J. J.; Zakrzewski, V. G.; Dapprich, S.; Daniels, A. D.; Strain, M. C.; Farkas, O.; Malick, D. K.; Rabuck, A. D.; Raghavachari, K.; Foresman, J. B.; Ortiz, J. V.; Cui, Q.; Baboul, A. G.; Clifford, S.; Cioslowski, J.; Stefanov, B. B.; Liu, G.; Liashenko, A.; Piskorz, P.; Komaromi, I.; Martin, R. L.; Fox, D. J.; Keith, T.; Al-Laham, M. A.; Peng, C. Y.; Nanayakkara, A.; Challacombe, M.; Gill, P. M. W.; Johnson, B.; Chen, W.; Wong, M. W.; Gonzalez, C.; Pople, J. A. Gaussian 03, revision C.02; Gaussian, Inc.: Wallingford, CT, 2004.

(31) Schlosser, F.; Kruger, S.; Rösch, N. *Inorg. Chem.* **2006**, *45*, 1480.

(32) Tissandier, M. D.; Cowen, K. A.; Feng, W. Y.; Gundlach, E.; Cohen, M. H.; Earhart, A. D.; Coe, J. V.; Tuttle, T. R., Jr. *J. Phys. Chem. A* **1998**, *102*, 7787 .

JP800209P